J Fluoresc (2010) 20:283–290
DOI 10.1007/s10895-009-0552-1

ORIGINAL PAPER

# Manipulation of Spontaneous Emission Dynamics of Organic Dyes in the Porous Silicon Matrix

**Abhinandan Makhal · Pushpendra Kumar · Peter Lemmens · Samir Kumar Pal**

Received: 15 June 2009 / Accepted: 28 September 2009 / Published online: 13 October 2009


**Abstract** The control of the spontaneous emission (SE) rate of dye molecules (4-dicyanomethylene-2-methyl-6-p-dimethylaminostyryl-4H-pyran (DCM) and Coumarin 523 (C523)) embedded in the Porous Silicon (PS) matrix has been studied using picosecond resolved fluorescence decay and polarization studies. We have shown that the SE rates of the two organic dyes embedded in the PS matrix depend on the relative positions of the emission maxima of the dyes with respect to electronic band gap energy of the PS matrix. We have also explored that the electronic band gap of the host PS matrix can easily be tuned by partial oxidation of the PS and the nature of SE of the embedded dyes can be tuned accordingly. The demonstrated retardation or enhancement of the spontaneous photon emission may enable the application of fluorescent organic molecules in PS matrix in several quantum optical devices including the realization of single photon sources.

**Keywords** Spontaneous emission from dyes · Dyes in porous silicon · Picosecond resolved emission · Time dependent polarization memory · Electronic band gap

A. Makhal · S. K. Pal (✉)
Unit for Nano Science & Technology, Department of Chemical, Biological & Macromolecular Sciences,
S. N. Bose National Centre for Basic Sciences,
Block JD, Sector III, Salt Lake,
Kolkata 700 098, India
e-mail: skpal@bose.res.in

P. Kumar · P. Lemmens (✉)
Institute for Condensed Matter Physics,
Technical University of Braunschweig,
Mendelssohnstr. 3,
38106 Braunschweig, Germany
e-mail: p.lemmens@tu-bs.de

## Introduction

Controlling the spontaneous emission (SE) of an emitter in the matrix of a photonic crystal has attracted significant attention in the field of quantum opto-electronic devices [1–4]. Applications are related to the development of various photonic devices like illumination displays, optical communication, solar energy and quantum information systems [4–7]. Several attempts to manipulate the SE dynamics of fluorescent quantum dots in various photonic crystal matrixes are reported in recent literature [3, 8]. In one of the studies CdSe quantum dots (QDs) are embedded in a titania inverse opal matrix and it has been demonstrated that the dynamics of SE of the QDs can be controlled by changing the lattice parameters of the host matrix [3]. Impregnation of organic dyes and their emission dynamics in solid state photonic crystal matrixes are also very interesting because of their applications in solar cells, optical wave guides, laser material and various sensors [7, 9, 10].

Recently, it has been demonstrated that density modulated porous silicon (PS) structures can act as a very useful photonic matrix to host various dyes in much easier ways [11, 12]. However, detailed investigations of the emission dynamics of the PS-impregnated dyes are sparse [13]. In one of the studies on a PS-Rhodamine composite, using a steady state polarization memory effect, it has been shown that the photo-excited dye undergoes an energy transfer reaction to the host matrix [12]. In the case of energy migration from the guest dye to the host matrix, enhancement of the SE rate is expected. However, the control of SE rate (enhancement and/or retardation) of different embedded organic dyes with different emission energies in a PS host matrix has not yet been reported. In a recent report it has been demonstrated that surface oxidation of the PS matrix effectively lowers the electronic band gap [14]. This is based on electronic states

that appear in the band gap of the smaller quantum dots (higher porosity) when a Si=O bond is formed. Changes in the electronic band-gap energy of the PS matrix with various degrees of porosity and surface oxidation are observed in this study [14]. The motive of our present work is to demonstrate a relatively less cumbersome way to control the SE of the guest organic emitters in a host PS matrix with tunable electronic band gap.

## Material and methods

Self supporting PS layers were formed by electrochemical anodization of highly doped p-type (100) oriented Si wafers with the resistivity of 0.01–0.02Ω cm in an HF based electrolyte [15]. After the porous layer reached the desired thickness of 25 μm, the anodization current was increased by a factor of 10 to release the porous layer from the bulk wafer underneath. The pore diameter and porosity of PS used in the present study are of the order of 10 nm and 50%, respectively, as determined by volumetric nitrogen sorption isotherms [16] at $T$=77 K and scanning electron microscopy.

Partially oxidized PS matrixes were obtained by immersing freshly prepared PS layers in hydrogen peroxide ($H_2O_2$) for 24 h and drying under vacuum. Here we have investigated the effect of oxidation of the matrix on the emission of the guest organic dyes. This work refers to freshly prepared, pristine PS and $H_2O_2$ oxidized PS as unoxidized (PS) and partially oxidized (OX-PS) matrixes, respectively. It has to be noted that fresh PS offers relatively strong photoluminescence due to confinement in the remaining Si crystallites surrounding the pores. However, intentional oxidation upon treatment with $H_2O_2$ or unintentional oxidation due to exposure to open air reduces the emission of the PS matrix [14, 17]. A systematic study on the rate of SE of the dye molecules upon controlled oxidation of the PS matrix is our future plan.

In order to compare the SE dynamics of the dyes in the PS matrix with the respective dynamics on non-porous optically transparent media, we have also studied thin films of the dyes on quartz plates. All samples (PS and quartz) were immersed for 5 h in a mixture of individual dye solutions (DCM[18] and C523[19]) in chloroform. Then the PS-samples were rinsed in chloroform in order to

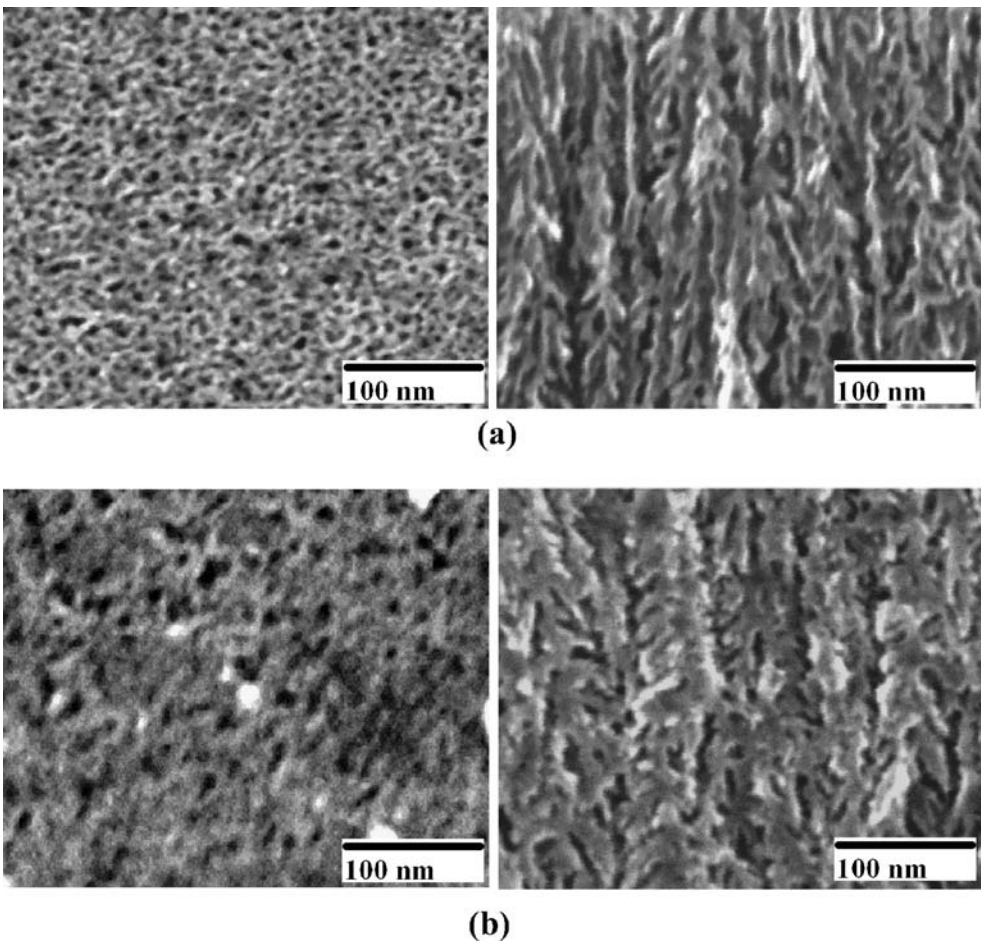


**Fig. 1** **a** SEM image of the surface and cross section view of freshly prepared porous silicon (*PS*) **b** SEM image of the surface and cross section view of the partially oxidized porous silicon (*OX-PS*)

remove all the residual dye molecules at the top surface of the samples. Finally, both dyes in PS and on quartz were dried for 2 h in a lyophilizer (Thermo LL1500) under vacuum. The cross sectional structure and surface morphology of as prepared and partially oxidized PS sample were investigated by using a field emission-type scanning electron microscope (FE-SEM; JEOL. Ltd., JSM-6500F).

For the emission and excitation measurements a Jobin Yvon Fluoromax-3 spectrophotometer was used. Picosecond resolved emission dynamics were investigated using a Lifespec Spectrometer (Instrumental Response Function, IRF ~61 ps, excitation at 375 nm) from Edinburgh Instruments (UK). All spectroscopic measurements were performed at room temperature. We have used a high-pass optical filter (420 nm) in order to avoid interference of the excitation light in the emission transients. The observed fluorescence transients are fitted by using a nonlinear least square fitting procedure to a function $(X(t) = \int_0^t E(t')R(t-t')dt')$ comprising of convolution of the IRF ($E(t)$) with a sum of exponentials $(R(t) = A + \sum_{i=1}^{N} B_i e^{-t/\tau_i})$ with pre-exponential factors ($B_i$), characteristic lifetimes ($\tau_i$) and a background ($A$) [20]. Relative concentration in a multi-exponential decay is finally expressed as $C_n = \frac{B_n}{\sum_{i=1}^{N} B_i} \times 100$. The quality of the curve fitting is evaluated by reduced chi-square and residual data. The average time constant $\tau_{av}$ of a multi exponential fluorescence decay is estimated as $\tau_{av} = \sum_{i=1}^{N} C_i \tau_i$.

## Results and discussion

Figure 1a shows SEM micrographs of top and crossectional views of the PS matrix. The larger mesopore structures are easily observed in the SEM imaging. The pores lie along the perpendicular direction to the Si surface and have

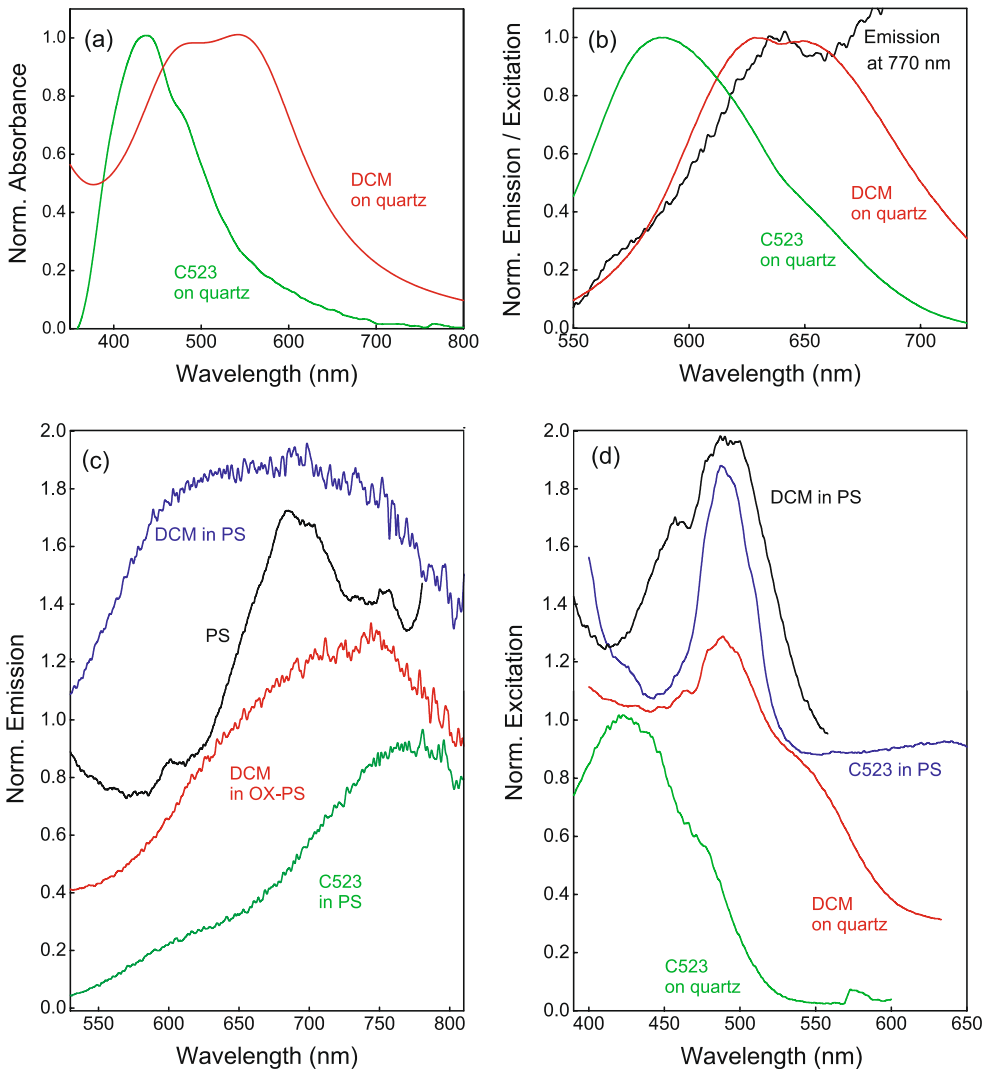


**Fig. 2** **a** Absorption spectra of C523 and DCM on quartz **b** Emission spectra of C523 and DCM on quartz. The excitation spectrum of PS matrix at 770 nm emission wavelength is shown. **c** Emission spectra of C523 and DCM in PS. The emission spectrum of the PS matrix is also shown. **d** Excitation spectrum of C523 on quartz and in PS (*upper*) and excitation spectrum of DCM on quartz and in PS (*lower*)

diameters ~10–12 nm. The pores themselves are heavily branched and their visible characteristics correspond to a 'fir tree' structure. The longer mesopore structures are also easily seen in the cleaved cross-section of the material by use of SEM imaging. $H_2O_2$ treatment of PS layers of this type leads to considerable oxidation at the pore wall surface, which is clearly evident from the top view and also cross section view Fig. 1b.

Figure 2a represents the normalized absorption spectra of C523 and DCM on the quartz plate. Figure 2b shows the excitation spectrum (emission at 770 nm) indicative of a distribution of electronic absorption energies of the host PS matrix in absence of guest organic dyes. The spectrum indicates an electronic absorption band around 640 nm (~1.94 eV). A strong overlap of the PS-absorption band with the emission spectrum of DCM on quartz (emission at 645 nm; ~1.92 eV) is also evident. On the other hand the emission peak of C523 (at 590 nm, ~2.1 eV) at a relatively higher energy state has a relatively lower spectral overlap with the PS absorption band. Figure 2c shows the emission spectra of the PS-embedded dyes. Here it is expected that both dyes transfer their excited state energy to the host PS matrix. Relatively poor SNR (signal to noise ratio) in the emission spectra of the embedded dyes with respect to that on the quartz plate (Fig. 2b) are indicative of emission intensity quenching in the PS-matrix. The emission of the PS-matrix (black) is also shown for comparison. The emission spectrum of DCM in the pristine (unoxidized) PS matrix shows (blue) a broad emission band with an insignificant apparent shift is the emission peak compared to that on the quartz surface. However, the DCM emission in the OX-PS shows significant red shift peaking at 770 nm. It has to be noted that the emission band of the DCM is in close proximity to that of the electronic excitation of the PS-matrix. On the other hand the excitation band of the OX-PS is expected to have a lower energy than that of the PS-matrix[14].

Our observation clearly indicates the role of the band gap of the host PS with respect to the transition energy of the guest organic dyes on the emission energy of the dye molecules. The emission spectrum of C523 in the PS matrix shows a red shift. However, the change in the emission pattern of C523 in the OX-PS compared to that in the PS is found to be insignificantly small. In order to investigate the effect of overlap of the electronic band of the host PS with that of the guest dyes in the emission properties of the dyes, we have compared the excitation spectra of the dyes on the quartz surface with those in the PS-matrix. As shown in Fig. 2d, C523 in the PS-matrix reveals significant red shift compared that on the quartz surface. The observation is consistent with the fact that C523 is adsorbed at the inner surface of the PS-pores and emission is coming from bound C523 dyes. Similar conclusion has been made to explain excitation spectra of the dye 9 AC at a $ZrO_2$ surface[21]. The excitation spectrum of DCM in the PS matrix is similar to that on the quartz surface. The observation along with the significant decrease in the quantum yield of the DCM molecule in the PS matrix compared to that of on the quartz surface, may be rationalized that the emission is from a very small fraction of DCM molecules, which are not adsorbed in pores but stuck

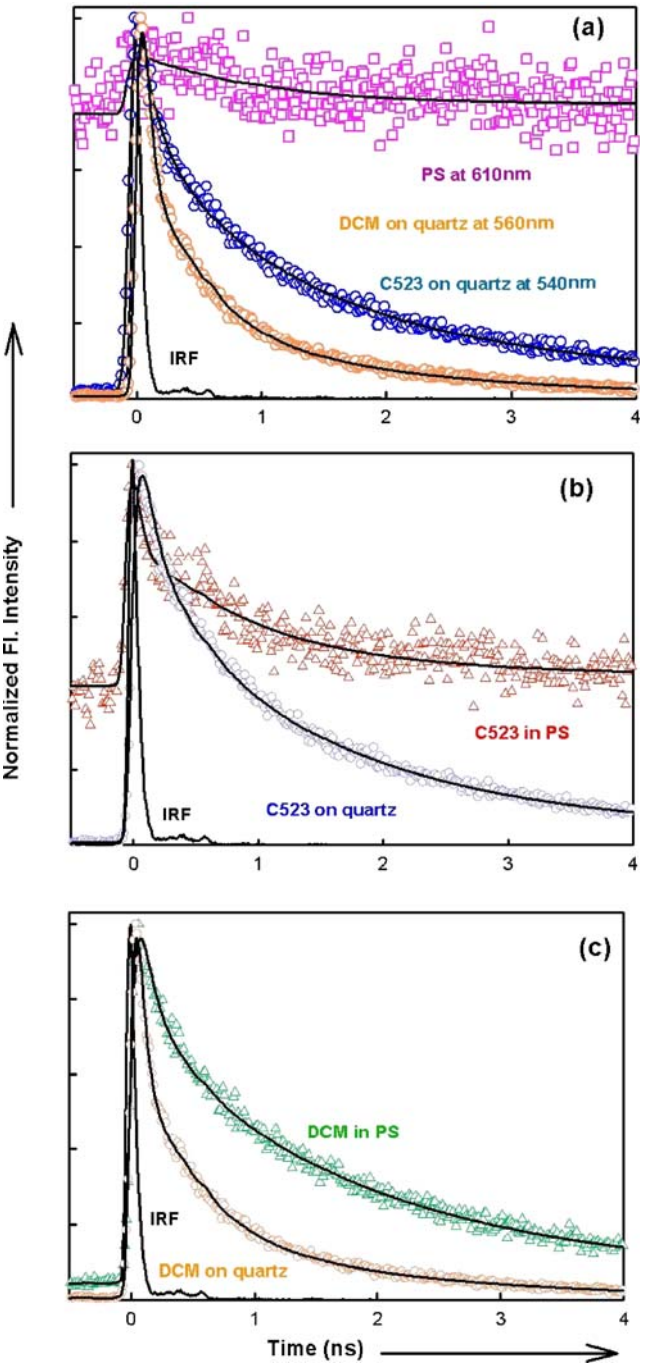


**Fig. 3** **a** Picosecond resolved emission transients of C523 and DCM on quartz. The transient of the PS matrix is shown for comparison. **b** Emission transients of C523 on quartz and in the PS matrix at 590 nm. **c** Emission transients of DCM on quartz and in the PS matrix at 590 nm

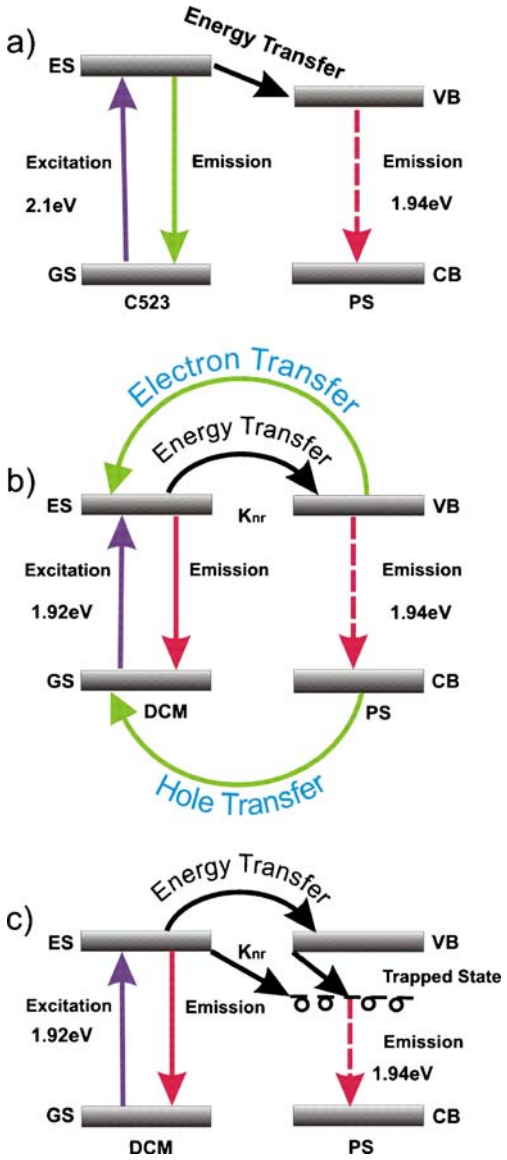


**Scheme 1** Possible photophysical processes of the embedded dyes C523 and DCM in the PS and OX-PS matrices are schematically presented. **a** Conventional excited state energy transfer from C523 to the host PS matrix is shown. Here emission from the system contains a de-excitation of the guest C523 and host PS as indicated by *solid arrows*. **b** The emission of embedded DCM in the PS matrix is presented. Here, the emission from the host PS matrix is quite forbidden because of the carrier trapping from PS to DCM molecule as indicated by *dotted arrow*. **c** The mechanism of the relatively faster fluorescence decay of DCM in OX-PS matrix compared to that on the quartz surface is shown. Direct/indirect energy transfer from DCM to the host matrix is shown. Insignificant emission from the host matrix is also indicated by a *dotted arrow*

at the surface of the PS. An alternative explanation for the insignificant shift in the excitation spectrum of DCM dye in the PS matrix could be due to the similarity of "band energy" of the dye with the host matrix.

The dynamical behavior of the SE of the dye molecules is evident from the data shown in Fig. 3. In Fig. 3a, time dependent SE of C523 and DCM on quartz plate are given. In the same figure, the emission dynamics of the PS-matrix is demonstrated indicating insignificant apparent decay (15 ns) at 610 nm in our experimental time window, associated with significant baseline offset. This observation is consistent with the very long excited state lifetime of the PS luminescence (~10 μs) [22]. In our experiment the repetition frequency of the excitation laser is 5 MHz, i.e. the time window between two successive excitation pulses is 0.2 μs. Figure 3b and c show emission decays (at 590 nm) of the dyes in the PS matrix and the emission decays of the dyes on a quartz plate at the same emission wavelengths.

Numerical fitting of the emission decay of C523 in PS matrix reveals 55 ps (77%), 1.6 ns (17%), 7 ns (6%) with an average excited state lifetime of 800 ps. The elevated baseline in the fluorescence transient is indicative of the interference of luminescence from the host PS matrix in the C523 emission. The emission decay of the C523 on the quartz plate shows an average lifetime of 1.60 ns (258 ps (26%), 1.50 ns (26%), 4.2 ns (16%)). On the other hand the average lifetime of DCM in the PS matrix is 1.20 ns (175 ps (48%), 1.50 ns (38%), 3.8 ns (14%)), which is slower than that on the quartz plate; 280 ps (46 ps (70%), 437 ps (23%), 1.95 ns (7%)). The insignificantly small baseline offset in the emission transient rules out a possible interference of PS luminescence in the DCM emission. From Fig. 3b and c, the enhancement of SE of C523 and retardation of SE of DCM, respectively, compared to those on quartz plates are clearly evident.

The above observation can be rationalized in the following model (Scheme 1). The emission maximum of the C523 at 590 nm is (at 2.1 eV; 81.08 $k_BT$) higher than the absorption band of the host matrix at 640 nm (1.94 eV; ~74.9 $k_BT$). Thus it is expected that dipole radiation of

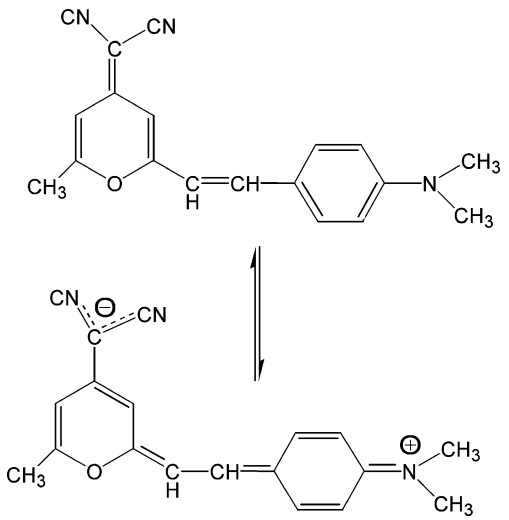


**Scheme 2** The resonance structure of the DCM molecule is shown. Possible carrier (electron and hole) trapping centers are given

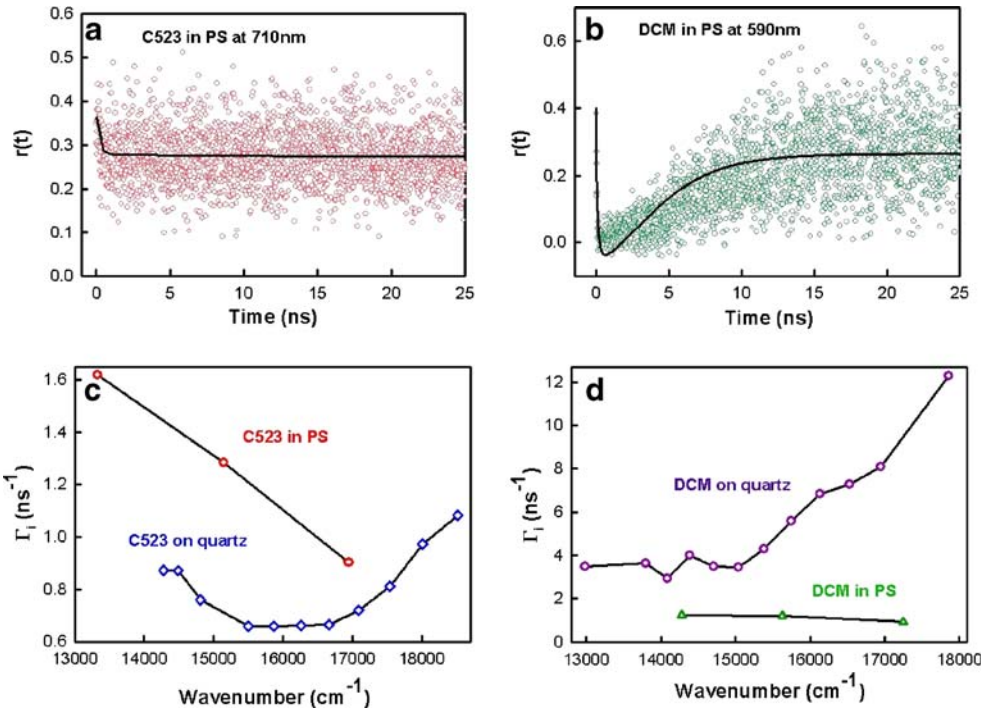


**Fig. 4** Polarization memory decay, r(t) of C523 at 710 nm (**a**) and DCM at 590 nm (**b**) in PS. *Solid black lines* are numerical fitting (see text). **c** Measured SE decay rates of C523 in PS matrix collected at 590 nm, 650 nm and 765 nm, and C523 on quartz collected from 560 nm to 770 nm with 15 nm intervals. **d** Measured SE decay rates of DCM in the PS matrix collected at 580 nm, 670 nm and 700 nm, and DCM on quartz collected from 540 nm to 700 nm with 15 nm intervals. *Solid black lines* are guides to the eyes

C523 can easily be migrated to the host matrix with lower electronic energy, showing a much faster decay component in the SE dynamics (Scheme 1(a)). On the other hand the emission maximum of DCM at 645 nm (1.92 eV; ~71.43 $k_BT$) is similar to that of the absorption of the PS matrix (absorption peak at 640 nm) with an insignificant difference between the two levels less than $k_BT$ (0.83 $k_BT$). Therefore the excited state energy of the DCM molecule can easily migrate to the PS-matrix, because of strong spectral overlap (Fig. 2b). Upon receiving excited state energy from a guest DCM molecule an electron hole pair (EHP) in the PS matrix is expected to be generated. The very long carrier lifetime in the host PS (~10 μs) eventually increases the possibility of trapping the carrier (electron and hole) in the DCM molecule[23]. Finally, the optical energy can be released due to a recombination of EHP in the DCM molecule itself (Scheme 1(b)). From the resonance level structure of the DCM molecule[24], the possibility of trapping electrons and holes simultaneously is very clear (Scheme 2). In a recent electroluminescence measurement of emission from DCM doped $Alq_3$ [tris-(8-hydroxyquinoline)] layers, the possibility of carrier trapping from host $Alq_3$ matrix to the DCM molecules (injected EHP recombination in the molecule) and overshooting of luminescence of the device due to electroluminescence of the DCM has been demonstrated.[23] The observed average lifetime of 1.2 ns of the DCM molecule in the PS matrix is consistent with the average lifetime of the molecule in a constrained medium[18, 25] and hence confirms confinement of the structural dynamics of DCM[24] in the PS pore compared to that on quartz surface.

Under these conditions there should be two types of DCM populations. One population may undergo an energy transfer with a ultrafast emission dynamics and another population should have a much longer lifetime due to electroluminescence of the DCM molecule. Such a situation is a primary case for a time resolved polarization memory (TRPM) analysis. The observed time resolved polarization memory effect [12, 18] $\left(r(t) = \frac{I_{\parallel}(t) - I_{\perp}(t)}{I_{\parallel}(t) + 2I_{\perp}(t)}\right)$ is in accordance with the above arguments, see Fig. 4a and b. The ultrafast decay of C523 in the porous matrix indicates an exciton migration to the host matrix ($\tau_1$~211 ps (95%), $\tau_2$~10 ns (5%)). The dip-rise nature of the TRPM of DCM in the PS matrix with two distinct DCM populations having two

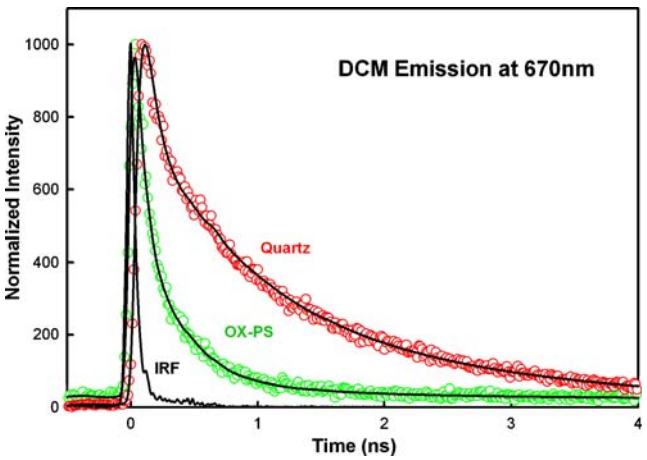


**Fig. 5** Picosecond resolved emission transients of DCM on quartz and in oxidized Porous Silicon (*OX-PS*) collected at 670 nm

different relaxation times ($\tau_1$~16 ps (82.5%), $\tau_2$~2 ns (17.5)) [18, 26], is a clear evidence of simultaneous energy transfer and electroluminescence due to back trapping of charge carriers. Our observation of the dip-rise nature of temporal polarization memory is consistent with that of another dye 9-anthracene-carboxylate in a $TiO_2$ host matrix [27], where back electron transfer from $TiO_2$ to the dye has been concluded to be responsible for the apparent rise in the polarization dynamics. The estimated excited state bleaching rates for the dyes C523 and DCM in the PS matrix are plotted in Fig. 4c and d. Here we estimate the excited state bleaching rate constants by inverting the average excited state lifetime of the dye molecules in the PS matrix and on the quartz plate ($\Gamma_i = \frac{1}{\tau_{av}}$). From the figures it is clear that the rate of excited state deactivation rates of C523 in PS matrix at various emission wavelengths are much faster than those on quartz surface indicating enhanced spontaneous emission in the PS matrix. On the other hand the excited state deactivation rates of DCM in the PS matrix in various emission wavelengths are slower than that on the quartz surface, which indicates retarded spontaneous emission in the matrix.

In order to further establish the fact that the proximity of the conduction band of the PS matrix is responsible for the trapping of EHP in the guest DCM, we have studied the dynamics of DCM emission in OX-PS (Fig. 5). As mentioned earlier, oxidation of the PS matrix generates a number of charge trapping states[14] and the effective band gap is reduced. Under this condition, OX-PS matrix is *not* expected to donate carriers to the guest DCM molecule. As shown in Fig. 5, the rate of SE from DCM in the OX-PS is enhanced compared to that on the quartz surface. The numerical fitting values of the emission decay of DCM in OX-PS matrix reveals 44 ps (73%), 255 ps (25%), 1.24 ns (2.5%) with an average excited state lifetime of 126 ps and that on quartz surface is 72 ps (73%), 500 ps (19%), 1.78 ns (8%) with an average excited state lifetime of 290 ps collected at 670 nm. It has to be noted that the retardation and enhancement of SE of DCM in the PS and OX-PS matrixes respectively are the consequence of gain and loss of excited state electrons compared to those on the quartz plate. The excited state deactivation rate can be estimated by comparing excited state lifetime of DCM in the PS and OX-PS matrixes with those on the quartz surfaces [28], $k = \frac{1}{\tau_{(DCM+PS/OX-PS)}} \pm \frac{1}{\tau_{(DCM)}}$. In the case of DCM in the PS matrix the carrier injection rate is estimated to be $2.74\times10^9$. The excited state deactivation rate in the OX-PS is $4.49\times10^9$, which is in the same order of the carrier injection rate in the PS matrix. This observation is summarized in Scheme 1(b) and is comparable to the case of C523 in PS matrix.

In conclusion, we have demonstrated an enhancement and retardation of SE from dyes with different emission wavelengths in the PS matrix. The fine tuning of the electronic band gap of the host matrix with respect to the emission energy of the guest organic dyes is the controlling factor of the SE from the dyes in the same matrix. The present study is an attempt to demonstrate such a control of SE of organic emitters embedded in a nanostructured matrix.

**Acknowledgement** We thank DST for a financial grant (SR/SO/BB-15/2007). AM thanks CSIR for a Junior Research Fellowship. The authors gratefully acknowledge Jörg Schmauch of Technische Physik, Universität des Saarland for SEM measurements. We acknowledge support by the Deutsche Forschungsgemeinschaft (DFG) and the NTH School "*Contacts in Nanosystems*".

## References

1. Bruchez M, Moronne M, Gin P, Weiss S, Alivisatos AP (1998) Semiconductor nanocrystals as fluorescent biological labels. Science 281:2013–2016
2. Brus LE (1984) Electron–electron and electron-hole interactions in small semiconductor crystallites: the size dependence of the lowest excited electronic state. J Chem Phys 80:4403–4409
3. Lodahl P, Driel AFV, Nikolaev IS, Irman A, Overgaag K, Vanmaekelbergh D, Vos WL (2004) Controlling the dynamics of spontaneous emission from quantum dots by photonic crystals. Nature 430:654–657
4. Noda S, Fujita M, Asano T (2007) Spontaneous-emission control by photonic crystals and nanocavities. Nature Photonics 1:449–458
5. Schubert EF, Kim JK (2005) Solid state light sources getting smart. Science 308:1274–1278
6. Ziemelis K (1999) Display technology: glowing devolopments. Nature 399:408–411
7. Gratzel M (2001) Photoelectrochemical cell. Nature 414:338–344
8. Englund D, Fattal D, Waks E, Solomon G, Zhang B, Nakaoka T, Arakawa Y, Yamamoto Y, Vuckovic J (2005) Controling the spontenious emission rete of single quantum dots in a two-dimentional photonic crystal. Phys Rev Lett 95:013901–013904
9. Adibi A, Xu Y, Lee RK, Loncar M, Yariv A, Scherer A (2001) Role of distributed Bragg reflection in photonic-crystal optical waveguides. Phys Rev B 64:041101–041104
10. Povinelli ML, Loncar M, Ibanescu M, Smythe EJ, Johnson SG, Capasso F, Joannopoulos JD (2005) Evanescent-wave bonding between optical waveguides. Opt Lett 30:3042–3044
11. Anglin EJ, Schwartz MP, Ng VP, Perelman LA, Sailor MJ (2004) Engineering the chemistry and nanostructure of porous silicon Fabry-Pérot films for loading and release of a steroid. Langmuir 20:11264–11269
12. Chouket A, Elhouichet H, Oueslati M, Koyama H, Gelloz B, Koshida N (2007) Energy transfer in porous-silicon/laser-dye composite evidenced by polarization memory of photoluminescence. Appl Phys Lett 91:211902–211903
13. Zheng WH, Reece P, Sun BQ, Gal M (2004) Broadband laser mirrors made from porous silicon. Appl Phys Lett 84:3519–3521
14. Wolkin MV, Jorne J, Faucher PM (1999) Electronic and luminescence in porous silicon quantum dots: the role of oxygen. Phys Rev Lett 82:197–200
15. Kumar P, Hofmann T, Knorr K, Huber P, Scheib P, Lemmens P (2008) Tuning the pore wall morphology of mesoporous silicon from branchy to smooth, tubular by chemical treatment. J Appl Phys 103:024303–024306
16. Brunauer S, Emmett PH, Teller E (1938) Adsorption of gases in multimolecular layers. J Am Chem Soc 60:309–319
17. Cullis AG, Canham LT, Calcott PDJ (1997) The structural and luminescence properties of porous silicon. J Appl Phys 82:909–965

18. Sinha SS, Mitra RK, Pal SK (2008) Temperature dependent simultaneous ligand-binding in human serum albumin. J Phys Chem B 112:4884–4891
19. Pryor BA, Palmer PM, Chen Y, Topp MR (1999) Identification of dual conformers of Coumarin 153 under jet-cooled conditions. Chem Phys Lett 299:536–544
20. O'Conner DV, Philips D (1984) Time correlated single photon counting. Academic, London
21. Martini I, Hodak H, Hartland VG (1998) Effect of structure on electron transfer reactions between anthracene dyes and TiO2 nanoparticles. J Phys Chem B 102:9508–9517
22. Tischler MA, Collins RT, Stathis JH, Tsang JC (1992) Luminescence degradation in porous silicon. Appl Phys Lett 60:639–641
23. Ma WC, Lengyel O, Kovac J, Bello I, Lee SC, Lee TS (2004) Time-resolved electroluminescence measurements of emission from DCM-doped Alq3 layers. Chem Phys Lett 397:87–90
24. Guo H, Zhang X, Aydin M, Xu W, Zhu H, Akins LD (2004) Spectroscopy and dyanamics of DCM encapsulated in MCM-41 and Y zeolite mesoporous materials. J Mol Struct 689:153–158
25. Sarkar R, Shaw AK, Ghosh M, Pal SK (2006) Ultrafast photoinduced deligation and ligation dynamics: DCM in micelle and micelle-enzyme complex. J Photochem Photobiol B 83:213–222
26. Das TK, Mazumdar S (2000) Effect of Adriamycin on the boundary lipid structure of cytochrome c oxidase: pico-second time-resolved fluorescence depolarization studies. Biophys Chem 86:15–28
27. Martini I, Hodak J, Hartland VG, Kamat PV (1997) Ultrafast study of interfacial electron transfer between 9-anthracene-carboxylate and $TiO_2$ semiconductor particles. J Chem Phys 107:8064–8072
28. Robel I, Kuno M, Kamat PV (2007) Size-dependent electron injection from excited CdSe quantum dots into $TiO_2$ nanoparticles. J Am Chem Soc 129:4136–4137